Inorganica Chimica Acta 587 (2025) 122829

Contents lists available at ScienceDirect

Inorganica Chimica Acta

journal homepage: www.elsevier.com/locate/ica

Research paper

Electrochemical behaviour and DNA intercalation studies of novel antimicrobial *Bis* - Cu(II) substituted Dipyridophenazine complexes

Darren F. Beirne [a], Sean O''. Neill [a], Eithne Dempsey [a], Kevin Kavanagh [b], Diego Seamus Montagner [a], Stephen Barrett [a,*]

[a] Department of Chemistry, Maynooth University, Maynooth, Ireland
[b] Department of Biology, Maynooth University, Maynooth, Ireland

ARTICLE INFO

Keywords:
Copper(II)
Dipyridophenazine
DNA intercalation
Redox activity
Antimicrobial

ABSTRACT

The public health threat caused by antimicrobial drug resistance has led to research towards alternatives to current chemotherapeutics, with metal-based complexes providing an excellent and promising avenue. Cu(II) species are of particular interest in this area due to their redox properties that could interfere with and inhibit bacterial growth. Here, we report the synthesis and characterisation of four novel bis-Cu(II) substituted Dipyridophenazine complexes. The dypyridophenazine ligands (DPPZ) where synthesized with different substituents at the 11 position (i.e. NO_2, Br, CH_3 and CN) to evaluate the effect of the functionality with respect the redox and biological behaviour. The DNA intercalation properties together with a detailed electrochemical study of the complexes and of the ligands is reported. The toxicity of the complexes against Methicillin Resistant *Staphylococcus aureus* (MRSA) and the yeast *Candida albicans* was characterised and the promise of this family of complexes as novel anti-microbial drugs in a post-antibiotic age was demonstrated.

1. Introduction

The treatment of *Staphylococcus aureus* infections faces challenges due to the rise of methicillin-resistant *Staphylococcus aureus* (MRSA), coupled with the escalating increase in resistance to conventional antimicrobials. For this reason there has been renewed focus on developing innovative antimicrobial agents based on a metallic scaffold. [1] Despite the well-established stature of traditional organic antibacterial agents, metal complexes, particularly those containing a Cu(II) centre with two aromatic planar scaffolds ligands, present themselves a promising alternatives. [2] Over the past two decades, exhaustive investigations have been conducted into the antimicrobial properties of $[Cu(phen)]^{2+}$ compounds. [3–6] Specifically, copper complexes featuring planar chelating ligands, demonstrated inhibitory activity against the growth of *S. aureus* and MRSA. [7,8] Unfortunately, the role of planar ligands in the antimicrobial activity of corresponding metal-based drugs remains unclear. However it is well known that substituted aromatic ligands such as pyrazino[2,3-f][1,10]phenanthroline (DPQ), dipyrido[3,2-a:2′,3′-c] phenazine (DPPZ), and benzo[*i*]dipyrido[3,2-a:2′,3′-c]phenazine (DPPN), shown below (Fig. 1), have all displayed enhanced DNA interaction via intercalation and artificial nuclease activity. [9] However, linking these properties to antimicrobial effects has proven challenging. [10,11] Alternative pathways, such as mitochondrial membrane damage and p53 upregulation, have also been proposed. [12] Recently, the anti-microbial activity of *bis*- DPPZ metal complexes (including Cobalt, Nickel, Ruthenium and Copper) was analysed. [13,14] Cellular accumulation showed that the Ruthenium complex containing the DPPZ ligand accumulated into the cells up to nine times more with respect the antibiotic ampicillin, particularly in the Gram negative bacterium *Pseudomonas aeruginosa* which is known to be resistant to many anti microbials due to the low permeability of its outer layer. [15]

Coupled with the antimicrobial activity of these DPPZ ligands is their ability to act as DNA intercalators or DNA groove binders. [16] DPPZ itself has shown binding values of $K_b > 10^5\ M^{-1}$ [17] while some of its metal complexes have displayed values of $K_b > 10^6\ M^{-1}$. [16] Gupta et al. studied the DNA intercalation properties of *Bis*-$[Cu(DPPZ)_2(Cl)](Cl)$ and *Bis*-$[Cu(DPQ)_2(Cl)](Cl)$, using calf thymus DNA. [18] In this case, the copper core had attached a chlorine in the fifth coordination position. The DNA binding studies showed values of the same magnitude of that discovered in 2003. [19] Previous values of 2.8×10^4 K_b (M^{-1} bp) for compound *Bis*-$[Cu(DPPZ)_2(Cl)](Cl)$ have been shown but much

* Corresponding author.
E-mail address: stephen.barrett@mu.ie (S. Barrett).

https://doi.org/10.1016/j.ica.2025.122829
Received 18 February 2025; Received in revised form 27 June 2025; Accepted 28 June 2025
Available online 30 June 2025

higher values of 4.5×10^4 K_b (M^{-1} bp) were displayed for the *Bis*-[Cu(DPQ)$_2$(Cl)](Cl). This would suggest the angular orientation of the DPPZ ligands in the five-coordinate structure of *Bis*-[Cu(DPPZ)$_2$(Cl)](Cl) could reduce its ability for efficient binding to DNA now that the chlorine moiety was attached. Previous studies carried out within our research group have also displayed large binding values for a copper compound containing the DPPZ ligand. The group determined a value of 1.44×10^7 K_{app} (M^{-1} bp) for a steroid - DPPZ derived copper (II) complex in comparison to values $\sim 10^6$ for the other three compounds tested (with the ligands Phen, DPQ and DPPN). [20]

In this paper, we report the synthesis, characterisation, the DNA binding and the antimicrobial activity of a series of Cu(II) complexes functionalised with 11-substitutes DPPZ ligands (Fig. 2). The complexes have the formula [Cu(R-DPPZ)$_2$Cl]Cl where R is NO_2, CN, Br and CH_3. The aim of this work was to explore the effect of the substituent in the DPPZ scaffold in term of DNA intercalation and antimicrobial properties.

2. Material and methods

All reagents and reactants were purchased from commercial sources. The two sources used were Sigma Aldrich and Tokyo Chemical Industry. The phendione was synthetized as previously reported by our group. [21] All solvents were used without further purification.

NMR spectra were recorded on a Bruker Advance spectrometer with the probe at 293 K, operating at 500 MHz for the ^{1}H nucleus and 125 MHz for the ^{13}C nucleus. Proton signals were assigned with the help of 2D NMR experiments (COSY). All chemical shifts are in ppm. Infrared (IR) spectra were recorded in the region 4000–400 cm^{-1} on a Perkin Elmer precisely spectrum 100 FT/IR spectrometer. The solid samples were run using ATR. Elemental analyses (carbon, hydrogen, and nitrogen) were performed with a PerkinElmer 2400 series II analyser. ESI mass spectra were recorded in positive mode with an Agilent 6200 Series TOF LC/MS system. UV-VIS spectra were recorded in a Perkin Elmer precisely Lambda 35 UV/Vis spectrometer. Conductivity experiments carried out on a Jenway 4510 conductivity meter at 25 °C with a cell constant at K = 1.01. The meter was calibrated using a standard solution of KCl of 0.01 M.

2.1. Syntheses and characterisation

The syntheses and the characterisation of the four ligands and four novel complexes can be found in the supporting information.

2.2. Conductivity studies

The ionic structure of the compounds were determined by conductivity studies on complex **4a** in triplicate carried out in deionised H2O at 25 °C. After addition of the complex (0.2 mM) the conductance was monitored and recorded at intervals of 30 s from the time of addition until the conductivity stabilised ~35 μS. A series of titrations were then carried out where 5 L of AgNO3 aliquots were added every three minutes over a 70-min period until a total of 3.0 eq were present in the solution. The conductance was recorded every 3 min during the titrations until all 3.0 eq of the AgNO3 had been added. The data was extrapolated and graphed in excel (Fig. 1S).

2.3. UV–vis stability studies

The stability of the compounds was evaluated through UV–Vis at 5 μM in a mixture of DMSO/PBS 1/1, over a period of 7 days. The first set of experiments were run between 290 nm and 800 nm at a concentration of 5 μM while the second set were run in the range 560–900 nm at a concentration of 180 μM (required as the bands are weaker for the d-d transitions, Figs. 2S and 3S).

2.4. Ethidium bromide displacement assay

Ethidium bromide DNA displacement assays were carried out using an adapted procedure from literature. [21] A 1:1.60 ratio (DNA:EtBr) was prepared to completely saturate the DNA helix with EtBr. The apparent binding constant K_{app} were calculated according to the competitive binding model described in previous literature using eq. **(1)**. [21]

$$K_{app} = K_{EB}[EB]/[agent] \quad (1)$$

Solutions of Salmon testes (st) DNA in 10 mM phosphate buffer (pH 7.4) gave a ratio of UV absorbance at 260 and 280 nm of 1:1.60, indicating that the DNA was sufficiently free of protein. Its concentration was determined spectrophotometrically using the molar absorptivity of 6600 M^{-1} cm^{-1} (260 nm). Titrations were carried out by monitoring changes in the absorbance and emission spectra of the dye (10 μM) at pH 7.4 in 10 mM phosphate upon successive additions of aliquots of stDNA.

2.5. Electrochemistry

Ligands **1–4** and the corresponding copper(II) complexes **1a-4a** were analysed electrochemically using cyclic voltammetry (CV). All electrochemical analyses were conducted on a Solartron 1287 potentiostat using a platinum wire counter electrode, a Glassy Carbon electrode (GCE) working electrode and non-aqueous $Ag|Ag^+$ reference electrode. 2 mM solutions of each compound were prepared in 0.1 M $LiClO_4$ in DMF. The working electrodes were prepared by polishing with 1 μm microcrystalline diamond suspension on a micro-cloth, followed by rinsing in deionised water. All voltammograms were generated using deaerated solutions (i.e. N_2 bubbling for 10 min prior to analysis). Scan rate studies were conducted on ligands **1–4** and complexes **1a-4a** at 50, 100 and 200 mV/s and the effect of the lower cathodic potential limit was also evaluated. Table 1 displays the electrochemical parameters obtained for the complexes **1a-4a** and of the ligands **1–4**. Fig. 4 shows the overlaid CV for the complexes using a short potential range (cathodic limit off −1.0 V vs. $Ag|Ag^+$) and also shows the overlaid CV of the ligands using a long potential range (cathodic limit of −3.0 V vs. $Ag|Ag^+$). Figs. 5S in ESI shows the overlaid CV of the complexes using a long potential range (cathodic limit of −3.0 V vs. $Ag|Ag^+$). Finally, Fig. 6S examines the influence of reducing agent (2 mM Ascorbic Acid) on the

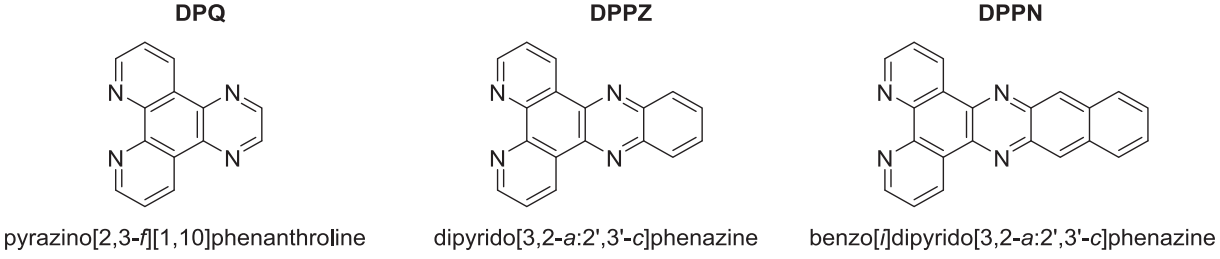

Fig. 1. Structures of the planar Dipyridophenazine ligands.

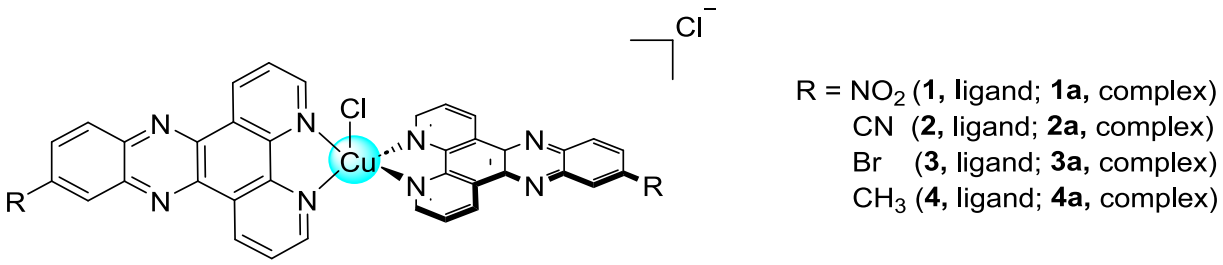

Fig. 2. Structures of *Bis*-[Cu(DPPZ-NO_2)$_2$Cl]Cl **(1a)**, *Bis*-[Cu(DPPZ-CN)$_2$Cl]Cl **(2a)**, *Bis*-[Cu(DPPZ-Br)$_2$Cl]Cl **(3a)**, *Bis*-[Cu(DPPZ–CH_3)$_2$Cl]Cl **(4a)**.

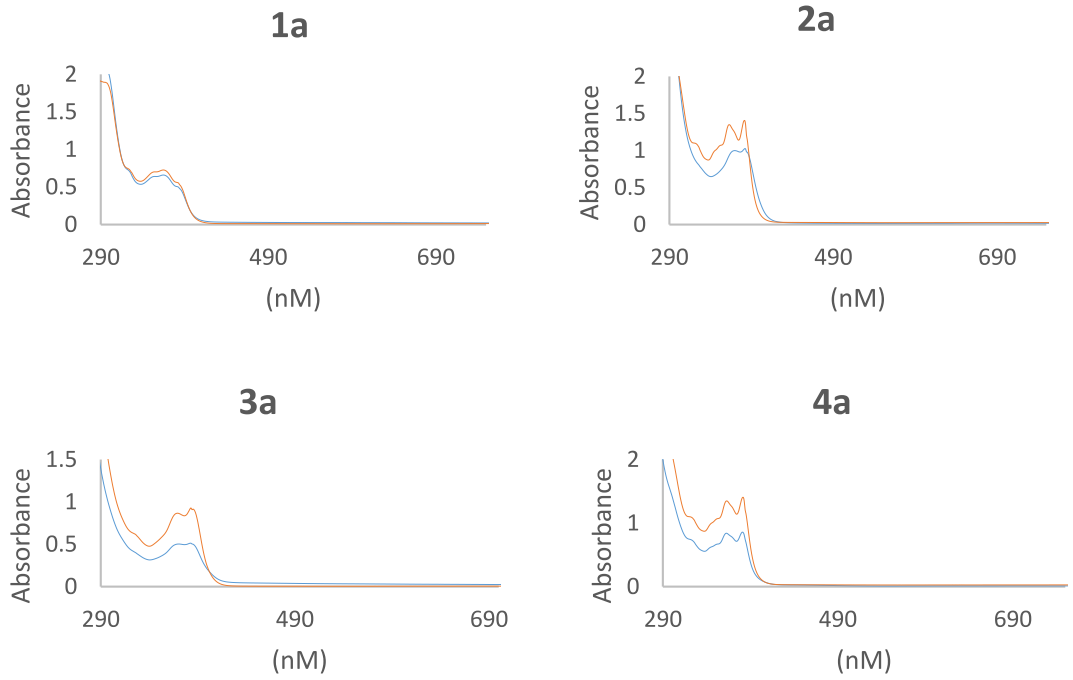

Fig. 3. UV–Vis spectra of the four Copper(II) complexes (DMSO/PBS 1/1) **1a – 4a** (5 μM). (•) after 1 h; (•) at day 7. Molar Extinction coefficients: **1a** = 1.04 × 10^{-6} M^{-1} cm^{-1}, **2a** = 1.61 × 10^{-6} M^{-1} cm^{-1}, **3a** = 1.33 × 10^{-6} M^{-1} cm^{-1}, **4a** = 1.51 × 10^{-6} M^{-1} cm^{-1}.

Table 1
Peak potentials for cathodic waves for ligands and complexes.

'R' Group	Ligand/ Complex	E_p^c/ V I	E_p^c/ V II	E_p^c/ V III	E_p^c/ V IV	E_p^c/ V V	E_p^a/ V	E_p^c/ V	ΔE_p / V	$E_{1/2}$ / V
NO_2	**1**	−1.12	−1.42	−1.87		−2.95				
	1a	−1.19	/	/	−2.38		−0.170	−0.312	0.142	−0.241
CN	**2**	−1.29	/	−1.84	/	−2.93				
	2a	−1.73	/	−2.25		−2.85	−0.188	−0.312	0.124	−0.250
Br	**3**	−1.23	−1.43	−1.94	/	/				
	3a	−1.31	/	−2.16	/	/	−0.167	−0.336	0.169	−0.252
CH_3	**4**	−1.24	−1.61	−1.93	−2.26	−2.5				
	4a	−1.24	−1.58	−2.14	/	−2.75	−0.212	−0.363	0.151	−0.287

complex **1a** electrochemistry (using $TBAPF_6$ as electrolyte in place of $LiClO_4$).

2.6. Antibacterial susceptibility assays

Bacteria (*Staphylococcus aureus*, methicillin resistant *Staphylococcus aureus* (MRSA and *Escherichia coli*) were sub-cultured from nutrient agar plates and grown in nutrient broth overnight in an orbital shaker at 37 °C and 200 rpm. The four final complexes and four free ligands were dissolved in 1 mL DMSO to give a stock concentration of 5 mg/mL. Nutrient broth (100 μL) was then added to each well of a 96 well plate. Each drug was serially diluted on the plate to give a concentration range 150–0.59 μg/mL. The bacteria used were grown overnight and the OD600 was adjusted to 0.1 (equivalent to cell density of 4 × 10^7/mL). The bacterial cells (100 μL) were added to each well and the growth was measured at 600 nm after 24 h at 37 °C using a spectrophotometer (BioPhotometer). All assays were performed in triplicate.

2.7. Antifungal susceptibility assay

The yeast *Candida albicans* was sub-cultured from a YEPD plate (Yeast extract (1 %), Bactopeptone (2 %), Glucose (2 %), Agar (2 %))

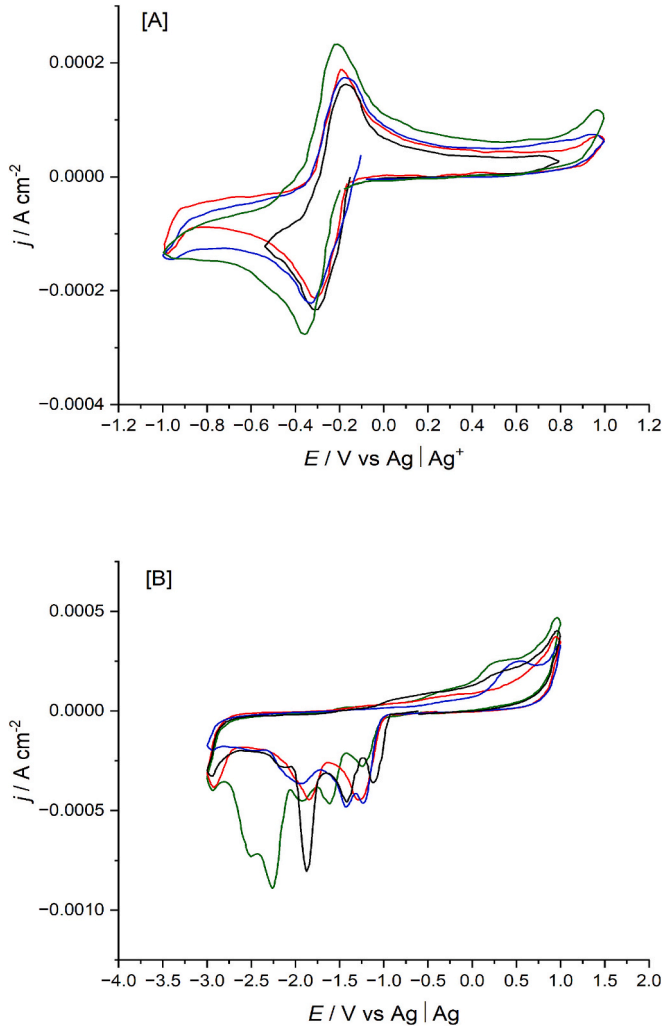

Fig. 4. [A]. CV of complexes **1a-4a** showing the Cu(II)/Cu(I) redox process over the range − 1.0 to 1.0 V vs Ag/Ag + at scan rate 50 mV/s at a glassy carbon electrode: (●) 1a; (●) 2a; (●) 3a; (●) 4a. [B]: Overlaid CVs for species (●) 1; (●) 2; (●) 3; (●) 4, potential range − 3.0 to 1.0 V vs. Ag/Ag^{+}.

and grown overnight at 37 °C and 200 rpm in in YEPD (Yeast extract (1 %), Bactopeptone (2 %), Glucose (2 %)) broth to the stationary phase (approx. 1×10^{8}/ml). Antifungal susceptibility assays were set up as described above by using YEPD broth. Yeast cells (1×10^{5} in 100 mL) were added to each well of the 96 well plate and the plates was incubated at 37 °C for 24 h under static conditions. Growth was quantified by measuring absorbance at 600 nm using a spectrophotometer (BioPhotometer). All assays were performed in triplicate.

3. Results and discussion

3.1. Synthesis and characterisation

The starting ligands (**1–4**) were obtained via a Schiff – base reaction between the corresponding substituted diamine and Phendione as previously reported by the group (Scheme 1). [22] Briefly, Phendione, which was synthesized in house using an adapted procedure [23] and the commercially available substituted diamine were reacted in a 1:1 ratio in either 100 % MeOH or a 50:50 mixture of EtOH: MeOH while refluxing for between 4 and 24 h. The precipitate was collected by filtration and taken back up in $CHCl_3$ then washed with brine and dried over Na_2SO_4 (See ESI).

The *Bis* – $[Cu(11\text{-R-DPPZ})_2(Cl)]Cl$ complexes were synthesized by suspending the previously formed ligands (**1–4**) in MeOH and refluxing in the presence of Copper (II) chloride dihydrate in a ligand: Copper salt ratio of 2.2: 1 for a duration of 4 h. The formed precipitate was collected by filtration and washed with $CHCl_3$, cold MeOH and finally H_2O to remove any remaining ligand and unreacted copper (II) salt, leaving the final Copper (II) complexes (**1a – 4a**, Scheme 1).

The complexes have been characterised by IR, UV-VIS and High-resolution Mass Spectroscopy and the purity was assessed via El. Anal. The ionic structure of the Copper (II) complexes were determined by conductivity via $AgNO_3$ titrations. Fig. 1S shows that the conductivity of **4a** was lowered upon titration with AgNO3, until 1 equivalents were added. Past 1 equivalent, the conductivity rose linearly which indicates the solution became more concentrated with $AgNO_3$ and no other inflection point was observed, demonstrating removal of only one chloride in the outer sphere of **4a**. The HRMS further verifies this as the ionisation observed for each complex is $[M\text{-}Cl^{-}]$. The UV–Vis spectra of the compounds in (DMSO/PBS 1/1)) show the intra ligand transitions π-π*, n-π* between 372 and 389 nm as strong peaks. The LMCT and MLCT are quite strong and overlap with the π-π*, n-π* transitions. These values are very close to those reported experimentally for the unsubstituted copper (II) bis complex of DPPZ of 355 nm. [24] This very broad peak which is due to the weak transitions in d - d is displayed at 710–760 nm (See ESI). The stability of the compounds was evaluated through UV-VIS (Fig. 3) in (DMSO/PBS 1/1) over a period of 7 days. Compound **1a** proved to be the most stable over the 7 days with minor changes observed in compounds **2a – 4a**. The molar extinction coefficients at their respective λ maxes are reported in Fig. 3.

3.2. Electrochemistry

The redox behaviour of the four ligands and of the four complexes was assessed using Cyclic Voltammetry, with the results displayed in **Fig. 4** and summarised in Table 2. **Fig. 4** displays the voltammogram generated over the potential range − 1.0 to 1.0 V for complexes **1a-4a**. Here, a quasi-reversible wave was observed for each complex, assigned to the $Cu^{2+/1+}$ redox process. The reduction potentials observed for each complex fell within the biological range (− 0.2 to −0.4 V), meaning they are likely to undergo reduction intracellularly. [25] The $Cu^{2+/1+}$ reduction potential for complexes **1a-3a** fell within a similar range (− 0.31 to − 0.29 V vs. Ag/Ag^{+}), while complex **4a** exhibited a slight shift in reduction potential in the cathodic direction (−0.36 V vs. Ag/Ag^{+}), indicating its slightly lower capability to be reduced. **4a** contains the only DPPZ ligand substituted with an electron-donating group (CH_3), probably explaining this discrepancy. No electrochemical data was observed in the literature for bis-DPPZ Cu(II) complexes, however, the obtained $Cu^{2+/1+}$ reduction potentials were in excellent agreement with what has been previously obtained by our group for heteroleptic Cu (II) complexes containing one DPPZ ligand and one estrogen-functionalised phenanthroline analogue (− 0.311 V) [26]. When the electrochemical behaviour of the complexes was compared to the free ligands (**Fig. 4**), a significant anodic shift in the E_c^p values for the DPPZ ligands was observed, indicating a reduced charge density present in the DPPZ ligands due to copper chelation. [27] Analyses conducted in presence and absence of ascorbic acid did not yield a significant difference in E_c^p for the $Cu^{2+/1+}$ process. However, addition of ascorbic acid resulted in an increased concentration of Cu(I), as extrapolated from the observed increase in oxidation current. The addition of reducing agent has little impact on the quasi-reversible nature of the $Cu^{2+/1+}$ redox process. [10]

3.3. DNA intercalation studies

The four copper (II) complexes proved to be far stronger DNA intercalators than their corresponding free ligands, with the exception of the Bromo complex **3a** (Fig. 5). This may be due to the Copper(II)

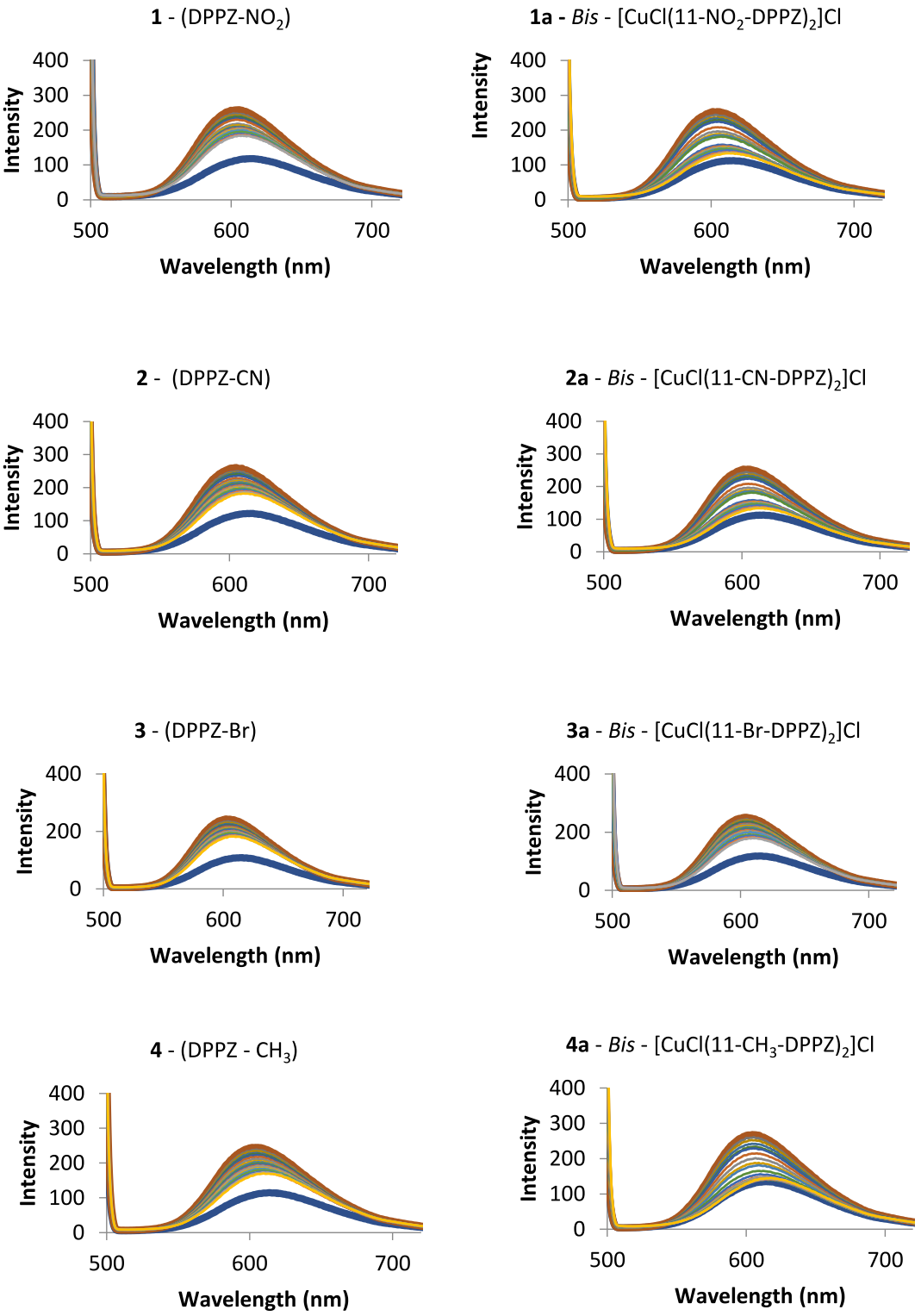

Fig. 5. Fluorescence quenching of the free ligands **1–4** (left) and corresponding Cu(II) complexes **1a-4a** (right).

nuclease centre having the ability to essentially lock the ligands into a distorted tetrahedral shape and allowing for a more stable intercalation into the DNA. However, in all cases more than 50 % relative quenching was observed and binding constants were able to be established (Table 2). The binding values were calculated using the % relative decrease of fluorescence at 50 % with the following equation.

The free ligands and the final metal complexes displayed binding constants in the region of $x10^6$ $(bp)^{-1}$ with two of the final complexes showing values in the $x10^7$ range. These values are very consistent with the values reported by Molphy et al. established for [Cu(phen)(DPPZ)] $(NO_3)_2$ in 2019. [17]

Although all eight of the compounds are effective intercalators, the strongest were found to be the copper (II) complexes with the cyano (**2a)** and the methyl (**4a)** substituents, with values of 1.82×10^7 $M(bp)^{-1}$ and 3.17×10^7 $M(bp)^{-1}$, respectively. In fact, complex **4a** displayed a marginally higher binding constant when compared to the unsubstituted

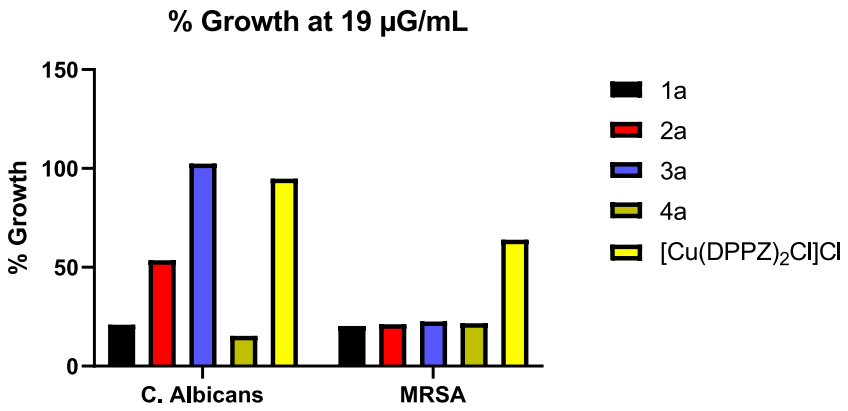

Fig. 6. MRSA % growth (Left) and *C. albicans* % growth (right) vs Copper(II) complexes at 19 µg / mL; (●) 1a; (●) 2a; (●) 3a; (●) 4a, (●) [Cu(DPPZ)$_2$Cl]Cl.

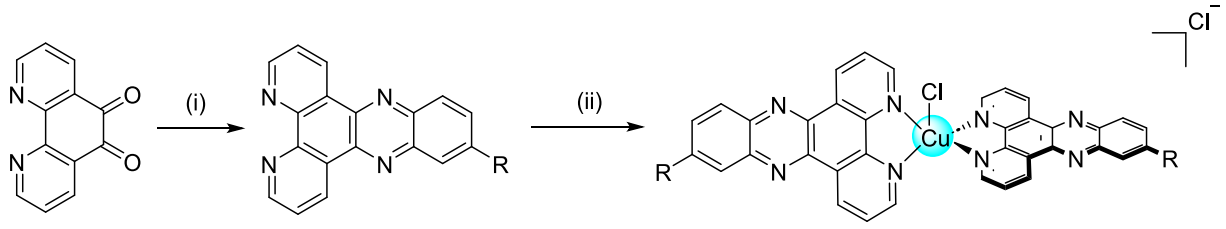

Scheme 1. Synthetic pathway to produce complexes **1a** – **4a.** (i) 4-R-benzene-1,2-diamine, MeOH/EtOH, 80–90 °C, 16 h, 48–87 % (ii) copper(II) chloride dihydrate, MeOH, reflux, 16 h, 64–74 %.

Table 2
Binding constants of ligands (**1–4**) and final copper (II) complexes (**1a – 4a).**

Compound	M(bp)$^{-1}$	Compound	M(bp)$^{-1}$
1	7.21×10^6	**1a**	8.08×10^6
2	8.09×10^6	**2a**	1.82×10^7
3	8.08×10^6	**3a**	7.21×10^6
4	9.21×10^6	**4a**	3.17×10^7
		[Cu(DPPZ)$_2$Cl] Cl	2.31×10^7

bis-[Cu(DPPZ)$_2$Cl]Cl control, which was found to have a binding value of 2.31×10^7 M(bp)$^{-1}$. The compounds with weaker interaction with the DNA are the NO_2 (**1a**) and Br (**3a**) derivatives, possibly due to the size of the bromine and nitro group atom that can prevent a tight intercalation.

3.4. Antimicrobial activity

The antimicrobial activity against the three bacteria and *C. albicans* was assessed as described in the Experimental part. The compounds displayed no activity against *S. aureus* and *E. coli* but were active against MRSA and *C. albicans*. The complexes at a concentration of 19 µg/mL resulted in approximately 80 % inhibition of MRSA growth (Fig. 6). Unlike what is reported in literature on anti-microbial activity of bis-DPPZ-Copper metal complexes (Co, Cu and Ni), the compounds **1–4** did not show activity against S.Aureus. [13] The activity against MRSA is similar to what is reported for Ruthenium DPPZ complexes with MIC values of 2 and 4 mg/L against MRSA252 and MRSA41, respectively [15]. Interestingly, the activity of complexes **1a-4a** in MRSA were all ~3 fold more active than the unsubstituted control (i.e. [Cu(DPPZ)$_2$Cl]Cl), highlighting an advantage to substitution of Cu(II)-DPPZ complexes in the 11th position to increase the activity. The activity against *C. albicans* has no current literature precedent for these kind of dypyridophenazine compounds. In the case of *C. albicans*, complex **1a** and **4a** inhibited growth by 80–90 %, complex **2a** inhibited growth by approximately 50 % but complex **3a** produced no inhibitory effect (Fig. 6). The activity of complexes **1a**, **2a** and **4a** are most impressive, especially when compared to the unsubstituted *bis*-[Cu(DPPZ)$_2$Cl]Cl, which showed no activity against *C. albicans*. Unfortunately, the complexes do not have comparable activity to positive control Amphotericin B (which has an impressive 80 % inhibition of *C. albicans* at just 0.41 µG/mL). However, these complexes may exhibit a better safety profile than amphotericin B, which is known to have severe side effects. Overall, these assays indicate that substitution in the 11th position of DPPZ can greatly enhance the anti-microbial activity of the Cu(II) complex.

4. Conclusions

In this work, four novel *bis*-Cu(II) complexes containing dypyridophenazine ligands with different substituents have been synthesized and characterised using IR, HRMS, UV-VIS and Elemental analyses. This novel family of complexes exhibit high binding affinity to calf thymus DNA, portraying their capabilities to act as strong DNA intercalators. The electrochemical redox behaviour, as examined by cyclic voltammetry, shows the ability of the complexes to be reduced in the cellular environment. The quasi-reversible nature of the redox process was proven and is consistent with the literature. Future studies to assess their capabilities to act as anti-cancer agents are to follow. The activity of the complexes against MRSA was examined and the antibacterial properties of each complex was significantly high, in line with similar compounds reported in literature. The high activity of the complexes against MRSA demonstrates their high potential to act as anti-microbial chemotherapeutics in a "post-antibiotic age". The complexes also showed inhibitor activity against *C. albicans*, that represents a novelty for these kind of DPPZ species. Interestingly, the complexes showed far greater activity against MRSA and *C. albicans* when compared to the unsubstituted control, demonstrating the importance of functionalisation in the 11th position. Further studies to elucidate their mechanism of action are to follow.

CRediT authorship contribution statement

Darren F. Beirne: Writing – review & editing, Writing – original

draft, Resources, Methodology, Investigation, Formal analysis, Data curation. **Sean O''. Neill:** Software, Investigation, Data curation. **Eithne Dempsey:** Writing – review & editing, Visualization, Software. **Kevin Kavanagh:** Writing – review & editing, Project administration, Methodology. **Diego Seamus Montagner:** Writing – review & editing, Writing – original draft, Project administration, Investigation. **Stephen Barrett:** Writing – review & editing, Writing – original draft, Supervision, Methodology, Conceptualization.

Declaration of competing interest

The authors declare that they have no known competing financial interests or personal relationships that could have appeared to influence the work reported in this paper.

Acknowledgements

DFB thankfully acknowledge support from Science Foundation Ireland (SFI): SFI 2012 Strategic Opportunity Fund (Infrastructure award 12/RI/2346/SOF) for NMR facilities.

Appendix A. Supplementary data

Supplementary data to this article can be found online at https://doi.org/10.1016/j.ica.2025.122829.

Data availability

Data will be made available on request.

References

[1] M.M. Cortese-Krott, M. Munchow, E. Pirev, F. Hessner, A. Bozkurt, P. Uciechowski, N. Pallua, K.D. Kroncke, C.V. Suschek, Free Radic. Biol. Med. 47 (2009) 1570–1577, https://doi.org/10.1016/j.freeradbiomed.2009.08.023.
[2] N.S. Ng, P. Leverett, D.E. Hibbs, Q. Yang, J.C. Bulanadi, M.J. Wu, J.R. Aldrich-Wright, Dalton Trans. 42 (2013) 3196–3209, https://doi.org/10.1039/C3CC41143E.
[3] T.S. Lobana, S. Indoria, A.K. Jassal, H. Kaur, D.S. Arora, J.P. Jasinski, Eur. J. Med. Chem. 76 (2014) 145–154, https://doi.org/10.1016/j.ejmech.2014.02.009.
[4] M. Geraghty, J.F. Cronin, M. Devereux, M. McCann, Biometals 13 (2000) 1–8, https://doi.org/10.1023/A:1009271221684.
[5] M. Geraghty, V. Sheridan, M. McCann, M. Devereux, V. McKee, Polyhedron 22 (1999) 2931–2939, https://doi.org/10.1016/S0277-5387(99)00201-6.
[6] L. Viganor, O. Howe, P. McCarron, M. McCann, M. Devereux, Curr. Top. Med. Chem. 17 (2017) 1280–1302, https://doi.org/10.2174/1568026616666161003143333.
[7] N.S. Ng, M.J. Wu, J.R. Aldrich-Wright, J. Inorg. Biochem. 180 (2018) 61–68, https://doi.org/10.1016/j.jinorgbio.2017.11.022.
[8] B.S. Creaven, D.A. Egana, D. Karcz, K. Kavanagh, M. McCann, M. Mahone, A. Noble, B. Thati, M. Walsh, J. Inorg. Biochem. 101 (2007) 1108–1119, https://doi.org/10.1016/j.jinorgbio.2007.04.010.
[9] N.S. Ng, M.J. Wu, C.E. Jones, J.R. Aldrich-Wright, J. Inorg. Biochem. 162 (2016) 62–72, https://doi.org/10.1016/j.jinorgbio.2016.06.006.
[10] Z. Molphy, A. Prisecaru, C. Slator, N. Barron, M. McCann, J. Colleran, D. Chandran, N. Gathergood, A. Kellett, Inorg. Chem. 53 (2014) 5392–5404, https://doi.org/10.1021/ic500914j.
[11] L. Viganor, A.C. Galdino, A.P. Nunes, K.R. Santos, M.H. Branquinha, M. Devereux, A. Kellett, M. McCann, A.L. Santos, J. Antimicrob. Chemother. 71 (2016) 128–134, https://doi.org/10.1093/jac/dkv292.
[12] Christophe Glorieux, Shihua Liu, Dunyaporn Trachootham, Peng Huang, Targeting ROS in cancer: rationale and strategies, Nat. Rev. Drug Discov. 23 (2024) 583–606, https://doi.org/10.1038/s41573-024-00979-4.
[13] P. Kumar, R.J. Butcher, A.K. Patra, Inorg. Chim. Acta 506 (2020) 119532, https://doi.org/10.1016/j.ica.2020.119532.
[14] A. Bolhuis, L. Hand, J.E. Marshall, A.D. Richards, A. Rodger, J. Aldrich-Wright, Eur. J. Pharm. Sci. 42 (2011) 313–317, https://doi.org/10.1016/j.ejps.2010.12.004.
[15] Z. Drulis-Kawa, J. Gubernator, A. Dorotkiewicz-Jach, W. Doroszkiewicz, A. Kozubek, Int. J. Pharm. 315 (2006) 59–66, https://doi.org/10.1016/j.ijpharm.2006.02.017.
[16] T. Phillips, I. Haq, A.J. Meijer, H. Adams, I. Soutar, L. Swanson, M.J. Sykes, J. A. Thomas, Biochemistry 43 (2004) 13657–13665, https://doi.org/10.1021/bi049146r.
[17] Z. Molphy, V. McKee, A. Kellett, Molecules 24 (2019) 4301, https://doi.org/10.3390/molecules24234301.
[18] T. Gupta, S. Dhar, M. Nethaji, A.R. Chakravarty, Dalton Trans. 44 (2004) 1896–1900, https://doi.org/10.1039/B404673K.
[19] M. Navarro, E.J. Cisneros-Fajardo, A. Sierralta, M. Fernández-Mestre, P. Silva, D. Arrieche, E. Marchán, J. Biol. Inorg. Chem. 8 (2003) 401–408, https://doi.org/10.1007/s00775-002-0427-2.
[20] S. Barrett, M. De Franco, A. Kellett, E. Dempsey, C. Marzano, A. Erxleben, V. Gandin, D. Montagner, J. Biol. Inorg. Chem. 25 (2019) 49–60, https://doi.org/10.1007/s00775-019-01732-8.
[21] Robert B.P. Elmes, Kim N. Orange, Suzanne M. Cloonan, D. Clive Williams, Thorfinnur Gunnlaugsson, J. Am. Chem. Soc. 133 (40) (2011) 15862–15865, https://doi.org/10.1021/ja2061159.
[22] S. Barrett, S. Delaney, K. Kavanagh, D. Montagner, Inorg. Chim. Acta 479 (2018) 261–265, https://doi.org/10.1016/j.ica.2018.04.054.
[23] C. Wang, L. Lystrom, H. Yin, M. Hetu, S. Kilina, S.A. McFarland, W. Sun, Dalton Trans. 45 (2016) 16366–16378, https://doi.org/10.1039/C6DT02416E.
[24] Z. Tan, J. Zhu, W. Ni, X. Liu, Y. Li, L. Tan, J. Biol. Inorg. Chem. 24 (2019) 721–731, https://doi.org/10.1007/s00775-019-01685-y.
[25] P. Zheng, A. Eskandari, C. Lu, K. Laws, L. Aldous, K. Suntharalingam, Dalton Trans. 48 (2019) 5892–5896, https://doi.org/10.1039/C8DT04706E.
[26] S. Barrett, M. De Franco, M. Donati, C. Marzano, V. Gandin, D. Montagner, Molecules 28 (10) (2023) 4112, https://doi.org/10.3390/molecules28104112.
[27] M. Magni, A. Colombo, C. Dragonetti, P. Mussini, Electrochim. Acta 141 (2014) 324–330, https://doi.org/10.1016/j.electacta.2014.07.086.